Mon. Not. R. Astron. Soc. **283,** 1–17 (1996)

The properties of the peculiar type Ia supernova 1991bg – I. Analysis and discussion of two years of observations

M. Turatto,[1,2] S. Benetti,[1] E. Cappellaro,[2] I. J. Danziger,[1] M. Della Valle,[3] C. Gouiffes,[4] P. A. Mazzali[5] and F. Patat[1,3]

[1] *European Southern Observatory, Karl-Schwarzschild-Strasse 2, D-8046 Garching bei München, Germany*
[2] *Osservatorio Astronomico di Padova, vicolo dell'Osservatorio 5, I-35122 Padova, Italy*
[3] *Dipartimento di Astronomia, Universitá di Padova, vicolo dell'Osservatorio 5, I-35122 Padova, Italy*
[4] *DAPNIA Sap/CE Saclay, F-91191, Gif-sur-Yvette Cedex, France*
[5] *Osservatorio Astronomico di Trieste, via GB Tiepolo 11, I-34131 Trieste, Italy*

Accepted 1996 May 20. Received 1996 March 29; in original form 1995 December 21

ABSTRACT

Observations of the peculiar type Ia supernova 1991bg in NGC 4374 collected at ESO La Silla and Asiago are presented and discussed. The photometric coverage extends for 530 d and the spectroscopy for the first 7 months after the explosion. The broad-band light curves in the early months have a narrower peak and a luminosity decline that is faster than other SNe Ia [14.6 and 11.7 mag $\times$ (100 d)$^{-1}$ in B and V respectively]. The R and I light curves do not show the secondary peak typical of normal SNe Ia. The SN is intrinsically very red [$(B-V)_{max}=0.74$] and faint ($B_{max}=-16.54$). The light curves flatten with age but remain significantly steeper [2.0 and 2.7 mag $\times$ (100 d)$^{-1}$ in B and V between 70 and 200 d] than the average. Consequently the *uvoir* bolometric light curve of SN 1991bg is fainter with a steeper decline than that of the normal SN Ia (e.g. 1992A). This object enhances the correlation that exists between the peak luminosity of SNe Ia, the decline rate and the kinetic energy.

Peculiarities are evident in the spectra at various phases. The continuum at maximum is very red and the photospheric expansion velocity extremely low. There are a number of unusual spectral features, in particular a broad absorption between 4200 and 4500 Å which is attributed to Ti II and the appearance, as early as one month after maximum, of nebular emission of possibly [Co III] λ5890–5908. Nevertheless, contrary to previous claims, the spectral evolution retains a general resemblance to that of other SNe Ia until the latest available observation (day 203). At this epoch one sees the typical emission features of SNe Ia at late times although they are significantly narrower (FWHM $\sim$ 2300 km s^{-1}). This facilitates the identification of most lines with forbidden emission of [Fe II], [Fe III] and [Co III]. The emission feature centred at about λ6590 is difficult to reconcile with the previous identification as Hα, unless asymmetries in the ejecta or ad hoc binary configurations are invoked.

This work suggests that the explosion energy was probably a factor of 3 to 5 lower than in normal SNe Ia. Whether this resulted from an explosion of a subChandrasekhar mass white dwarf (WD) is not unambiguously established.

Key words: supernovae: general – supernovae: individual: 1991bg – supernovae: individual: 1991F – supernovae: individual: 1986G – supernovae: individual: 1992K – supernova remnants.

1 INTRODUCTION

Supernovae of type Ia (SNe Ia) have been considered for decades and are still considered by some to be almost perfect distance indicators. Actually, some scatter in their photometric properties was suggested as early as the late 1960s (Pskovskii 1967, 1971; Barbon et al. 1973a), but it has been mostly attributed to photometric errors (e.g. Sandage & Tammann 1993).

However, in recent years the discovery of two extreme SNe Ia, 1991T and 1991bg, challenged the standard candle scenario for SN Ia, 1991T being brighter than the average SN Ia (Phillips et al. 1992; Ruiz-Lapuente et al. 1992; Mazzali, Danziger & Turatto 1995) and 1991bg significantly fainter (Filippenko et al. 1992; Leibundgut et al. 1993). The two supernovae (SNe) also showed distinctive spectral peculiarities which, however, might have gone unnoticed if only sparse observations had been gathered. Therefore, a question arises: are the samples of SNe Ia used as standard candles heavily contaminated by such extreme objects and how much such contamination affects the derived values of H_0 and q_0? The question has been further complicated by the recognition that even SNe Ia with very similar spectra can show a significant spread in absolute magnitude (Patat et al. 1996), which may correlate with the photometric evolution and even with the morphological type of the parent galaxy (Hamuy et al. 1995).

Supernovae of different intrinsic brightnesses have different probabilities of being detected, hence it is expected that the intrinsic fraction of faint SNe is higher than the actual percentage of discoveries. This has implications for the chemical evolution of the galaxies, since SNe Ia are thought to be a primary source of Fe-peak elements.

The goal of this paper is to present and discuss new photometric and spectroscopic observations of SN 1991bg, describing the evolution of this object until the late nebular stages and to highlight peculiarities and similarities compared with other SNe Ia. Some quantitative indications on the precursor star and the total amount of synthesized material will also be given.

2 OBSERVATIONS AND REDUCTIONS

2.1 Photometry

SN 1991bg was discovered on 1991 December 9.8 by R. Kushida (Kosai et al. 1991) about 1 arcmin south of the nucleus of the elliptical galaxy NGC 4374, which is located near the centre of the Virgo cluster.

The observations at the ESO La Silla and Asiago Observatories started soon after the discovery and continued for the next 7 months, until the Virgo cluster disappeared behind the Sun. Eventually the SN was detected 530 d after maximum.

The broad-band B, V and R photometry (together with two I-band observations) are listed in Table 1. Depending on the brightness of the object and on instrument schedule, several different telescopes were used. On photometric nights sequences of standard stars (Landolt 1992) were observed which allowed the determination of the colour equations of the photometric systems. These were in good agreement with the determinations by other authors. For calibrating the non-photometric nights, a local sequence was established around the galaxy. For the stars in common with the sequences of Leibundgut et al. (1993) and Filippenko et al. (1992), our measurements agree to within a few hundredths of a magnitude with those of the above authors.

Until 200 d the photometric measurements were performed with the ROMAFOT package, the utilization of which in the context of SNe has already been discussed (cf. Turatto et al. 1993). The errors in the SN magnitudes depend on the contrast of the star against the galaxy background, and were estimated to range from 0.05 at early epochs up to 0.2 mag at 7 months. In Fig. 1 our measurements are plotted together with those by Filippenko et al. (1992) and Leibundgut et al. (1993). It is evident that while at early epochs the agreement between the different sources is good, it becomes poor as the SN fades. In particular, at about 150 d our estimate appears 0.5 mag fainter than those of Leibundgut et al. (1993). Since the zero point is the same (the local sequences coincide), the inconsistency has to be attributed to the measuring technique. Both Leibundgut et al. and Filippenko et al. derived the SN magnitudes by means of aperture photometry but, while the former authors measured the background in an annulus around the SN, the latter ones, exploiting the symmetric surface brightness profile of the elliptical parent galaxy, subtracted the image of the galaxy rotated by 180° around the major axis.

Table 1. CCD photometry of SN 1991bg.

Date	JD[a]	B	V	R	I	Instr.
15/12/91	8605.85	14.87	14.11			NTT
31/12/91	8621.92		15.44			NTT
01/01/92	8622.84	16.82	15.57	15.04		0.9m
02/01/92	8623.84	16.81	15.62	15.16		0.9m
02/01/92	8623.85		15.67			NTT
03/01/92	8624.84	16.99	15.63	15.14		0.9m
05/01/92	8626.84	17.10	15.80	15.30		0.9m
07/01/92	8628.85	17.00	15.77			0.9m
10/01/92	8631.85		16.02			0.9m
15/01/92	8636.67	17.40	16.16			NTT
16/01/92	8637.67	17.38	16.32	15.92		NTT
17/01/92	8638.70	17.34	16.28			NTT
18/01/92	8639.60	17.47				NTT
04/02/92	8656.86	17.75	17.01	16.85		3.6m
05/02/92	8657.61	17.75	16.98	16.94		1.8m
05/02/92	8657.88	17.81	17.03	16.88		3.6m
06/02/92	8658.53	17.90	17.10	16.90		1.8m
25/02/92	8677.67	18.15	17.75	17.77		NTT
01/03/92	8682.75	18.35	17.93	17.84		2.2m
06/03/92	8687.55	18.55	18.00	17.90		1.8m
07/03/92	8688.54	18.55	18.01	18.05		1.8m
10/03/92	8691.50			18.20		NTT
08/04/92	8720.75	19.14	19.05	18.93	18.00	2.2m
04/05/92	8746.60	19.78	19.90	19.77	18.81	3.6m
03/07/92	8806.52	21.03	21.19	21.04		3.6m
23/01/93	9010.81		> 22.50	> 22.10		3.6m
06/03/93	9053.24		> 23.50			HST
26/05/93	9133.57		24.95			NTT

(*a*) +244 0000; NTT = New Technology Telescope + EMMI; 3.6-m = ESO 3.6-m + EFOSC; 2.2-m = ESO/MPI 2.2-m + EFOSC2; 1.8-m = Asiago 1.8-m + CCD camera; 0.9-m = Dutch 0.9-m + CCD camera; *HST* = *HST* + WFC + F555W.

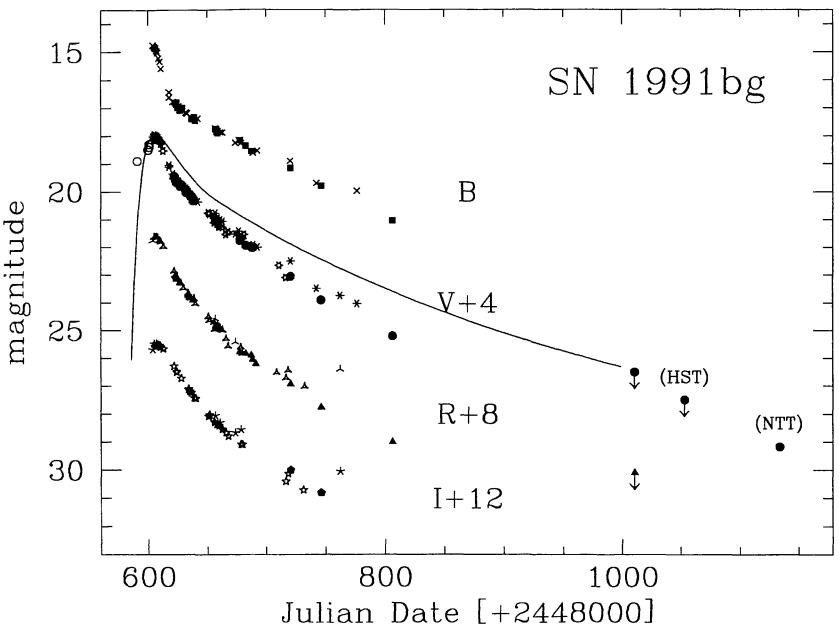

Figure 1. The light curves of SN 1991bg in the *BVRI* bands. Ordinates are *B* magnitudes while all other bands have been shifted down as indicated. The solid line is the *V* light curve of SN 1992A (Wheeler & Benetti 1996) adjusted to match the *V* maximum of 1991bg. Filled symbols are the observations presented here, starred symbols are from Filippenko et al. (1992), skeletal symbols are from Leibundgut et al. (1993) and open symbols from IAU Circulars.

We have tested the measurements of the SN magnitude with both of these methods: already at epochs earlier than 100 d the subtraction of annuli produced results dependent on the radii of the annuli, while the subtraction of the rotated galaxy gave results within a few hundredths of a magnitude of our ROMAFOT determination.

Based on the first, unsuccessful attempt to recover the SN, in 1993 January, upper limits for the SN magnitude were derived by placing increasingly fainter artificial stars at the precise position of the SN relative to nearby stars. The result was $V \geq 22.5$ and $R \geq 22.1$ mag. A somewhat fainter upper limit was obtained using an image taken with the Wide Field Camera (WFC) of the *Hubble Space Telescope* (*HST*) on 1993 March 6 in the F555W passband (very close to the standard *V*) and retrieved from the *HST* Archive. The exposure was not very long (300 s) and the frame was processed with the Routine Science Data Processing pipeline. Using both the internal calibration of the frame and a faint comparison sequence calibrated with our deep ground-based observations, we found $V \geq 23.5$ for the SN at this epoch.

Finally, a series of 17 exposures (total observing time 170 min) was obtained on 1993 May 26, i.e. 530 d after *B* maximum. The frames were flat-fielded, aligned and co-added into a single exposure in order to improve the signal-to-noise ratio. Although the seeing was not exceptional (1.15 arcsec) a stellar image was found within 0.1 arcsec from the expected position (Fig. 2). In this case, the SN magnitude was also measured using SNOOPY, a new software especially designed for SN photometry by one of us (FP). As for ROMAFOT, in SNOOPY the magnitude is derived by means of the point spread function fitting technique, but background fitting was improved and interactivity enhanced (Patat, in preparation). The resulting magnitude was $V = 24.95$. The error in the measurement was estimated by means of artificial star tests. The dispersion of the recovered magnitudes of 50 artificial stars positioned near the SN was rms = 0.40 mag.

2.2 Spectroscopy

The journal of the spectroscopic observations is given in Table 2, where the instrumentation and the spectral ranges are indicated. The spectra were calibrated in wavelength with adjacent spectra of comparison lamps and flux calibrated with spectrophotometric standard stars observed on the same nights. Different exposures obtained during the same night (or in consecutive nights at late epochs) with the same configuration have been co-added in order to increase the signal-to-noise ratio while those obtained with different gratings or grisms have been merged. When the SN broad-band photometry was available on the same night, the absolute flux calibrations of the spectra were checked. In most cases corrections were not needed, but, if necessary, corrections of the order of a few tenths of a magnitude were applied.

During the observations particular care was given to the accurate positioning of the slit, whose width was typically between 1.5 and 2 arcsec. When the spectra were obtained at large zenith distances the slit was aligned along the parallactic angle, otherwise a second exposure was taken with a wider slit (5–10 arcsec) in order to ensure that all the light from the object entered the slit. The spectral resolution was typically 10 Å at the NTT, and 12 Å at the 2.2-m, 20 Å at the 3.6-m and 22 Å at the 1.8-m telescopes. Composite spectra obtained by merging data from different equipment or configurations (e.g. grisms or gratings) may thus have different resolutions at different wavelengths. For instance, the spec-

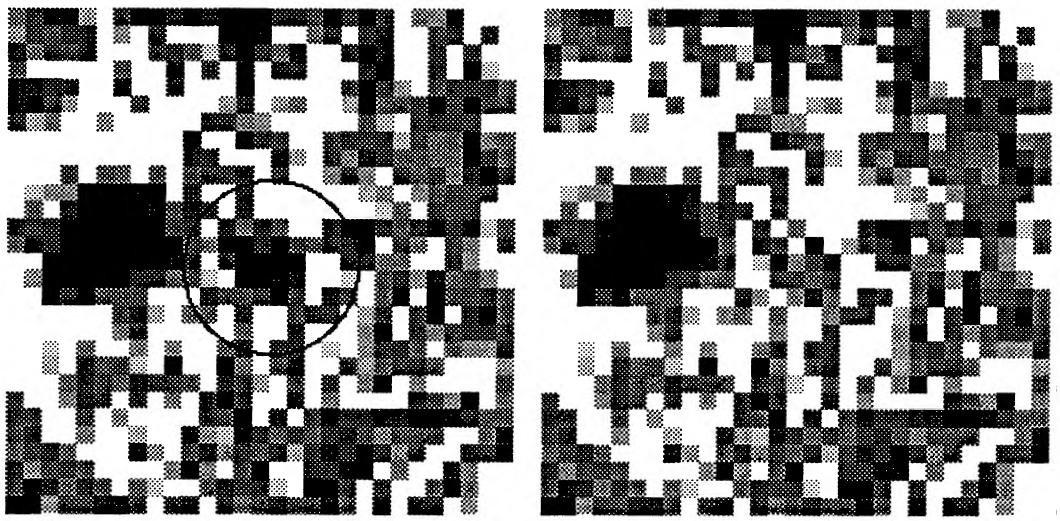

Figure 2. Co-added V image of SN 1991bg in NGC 4374 obtained on 1993 May 26 (i.e. 530 d after maximum) at the NTT (+ EMMI) (total exposure 170 min, seeing 1.15 arcsec). The left panel shows the co-added original frame once the smooth background of the parent galaxy has been subtracted ($\mu_V \sim 21.4$ mag arcsec^{-2}). The expected position of the SN has been encircled. The right panel shows the same area after the subtraction of the SN.

Table 2. Journal of the spectroscopic observations of SN 1991bg.

Date	phase[a] (days)	JD[b]	Wavelength range (Å)	Instrum.
14/12/91	0.7	8604.65	3650-9250	1.8m
15/12/91	1.6	8605.60	4030-9200	1.8m
15/12/91	1.9	8605.85	3880-8120	NTT
29/12/91	15.6	8619.57	4170-8450	1.8m
31/12/91	17.9	8621.88	4170-9800	NTT
02/01/92	19.5	8623.85	4170-7860	NTT
14/01/92	31.5	8635.54	3850-9420	1.8m
15/01/92	32.5	8636.54	6850-11000	1.8m
16/01/92	33.7	8637.67	4160-7950	NTT
28/01/92	45.6	8649.56	3560-9040	1.8m
01/02/92	49.8	8653.83	3560-7100	2.2m
04/02/92	52.7	8656.65	3560-9200	1.8m
04/02/92	52.9	8656.87	3600-6720	3.6m
13/02/92	61.6	8665.56	4050-8410	1.8m
25/02/92	73.7	8677.67	5400-6500	NTT
01/03/92	78.8	8682.79	4470-8200	2.2m
10/03/92	87.5	8691.50	4200-10000	NTT
08/04/92	116.7	8720.71	3560-9100	2.2m
04/05/92	142.6	8746.60	3730-6900	3.6m
03/07/92	202.5	8806.52	3770-6900	3.6m

(*a*) from B maximum (JD 244 8604.0); (*b*) + 244 0000; NTT = New Technology Telescope + EMMI; 3.6-m = ESO 3.6 m + EFosc; 2.2 m = ESO/MPI 2.2 m + EFOSC2; 1.8 m = Asiago 1.8 m + B&C.

trum at $t = +117$ d has a resolution of about 12 Å between 4470 and 8420 Å, and about 30 Å outside this range.

3 LIGHT CURVES

The light curves of SN 1991bg in the first months after maximum, already discussed by Filippenko et al. (1992) and Leibundgut et al. (1993), are updated in Fig. 1 with the inclusion of our new data. It is confirmed that the photometric evolution of SN 1991bg differs from that of normal SNe Ia: the maximum peak is narrower and the luminosity decline faster. Pre-maximum observations are scant and quite uncertain, therefore little can be said about the rise to maximum light. Our best estimates of the epochs and magnitudes at maximum are reported in Table 3 and are in good agreement with previous estimates.

The light curves of SN 1991bg in the first 2 months after maximum are compared in Fig. 3 to those of the normal SN Ia 1994D and of the somewhat peculiar SN Ia 1986G. The general behaviour of SNe Ia, showing a slower luminosity decline in the red than in the blue, holds also for SN 1991bg which, however, shows the steepest initial luminosity decline rate, namely 14.6 and 11.7 mag $\times$ (100 d)$^{-1}$ in B and V, respectively, to be compared with 12.5 and 7.2 mag $\times$ (100 d)$^{-1}$ measured in SN 1994D (Patat et al. 1996). The secondary maximum, which is quite pronounced in the I light curve of SN 1994D, is absent in SN 1991bg.

The light curve evolution of SN 1986G is also faster than that of SN 1994D [12.8 and 8.6 mag $\times$ (100 d)$^{-1}$ in B and V respectively] albeit not as fast as SN 1991bg (cf. Fig. 3). Unfortunately, the R and I light curves of SN 1986G are not available, and so a comparison with SN 1991bg, which departs strongly from the standard SNe Ia in these bands, is not possible but neither SN shows the secondary maxima in the near-IR typical of normal SNe Ia (Frogel et al. 1987; Porter et al. 1992).

As early as 15 d after maximum, the B light curve of SN 1991bg begins a slower decline, while at increasingly redder wavelengths the change of slope occurs later and is less

Table 3. Basic photometric data of SN 1991bg.

	B	V	R	I	bol
			MAXIMA		
J D (+2448000)	~ 604.0	605.5 ± 1.0	606.0 ± 1.0	608.0 ± 1.0	605.0 ± 1.0
mag	$\sim 14.75 \pm 0.1$	13.96 ± 0.05	13.63 ± 0.05	13.50 ± 0.05	
abs mag*	-16.54 ± 0.32	-17.28 ± 0.31	-17.58 ± 0.31	-17.68 ± 0.31	-16.50 ± 0.34
$\log L$ [erg s^{-1}]					42.20 ± 0.14
		FADING RATES $[mag \times (100d)^{-1}]$ (phase range [days])			
early	14.6(3-14)	11.7(6-14)	9.4(6-24)	7.3(9-24)	9.1(4-20)
intermediate	2.6(17-59)	4.2(17-64)	4.6(30-59)	4.8(30-64)	3.6(30-70)
late	2.0(70-203)	2.7(70-203)	2.6(70-203)	2.7(75-143)	2.6(70-203)
very late		1.2(203-530)			
		BENDING POINTS			
epoch$_1$ [days]	15	17	24	28	22
$\Delta(m)_1$ [mag]	1.95	1.44	1.77	1.50	1.70
epoch$_2$ [days]	60	60	68	65	70
$\Delta(m)_2$ [mag]	3.25	3.34	3.87	3.30	3.50

COLORS	$(B-V)$	$(V-R)$	$(V-I)$
day 0 (B max)	0.74	0.25	0.33
day 15–17	1.45	0.60	1.25

*$E(B-V)=0.05$, $\mu=31.09$.

evident. Therefore, the value of $\Delta(m)_1$ given in Table 3 for the B band corresponds to the parameter $\delta m_{15}(B)$ defined by Phillips (1993). Our determination is in good agreement with his estimate even after the inclusion of our new photometry.

3.1 The photometric evolution

Previous analyses have shown that the light curve of SN 1991bg can be well approximated by three segments spanning from days 4 to 20, 20 to 60 and 60 to 200, respectively. The inclusion of our new data changes the positions of the bending points slightly with respect to earlier determinations (Filippenko et al. 1992; Leibundgut et al. 1993). The epochs of the bending points and slopes [in units of mag $\times$ (100 d)$^{-1}$] of the three segments are given in Table 3. As we will argue later, the fast evolution of the early light curve is indicative of a small ejecta mass.

The new observations of Table 1 are especially important since they constrain the late-time photometric behaviour of SN 1995bg. 2 months after maximum, the second bending point in the light curves marks the beginning of the radioactive tail when then remains linear until at least day 200 (Table 3). Again the luminosity decline rate of SN 1991bg in this phase is significantly faster than those of all other well-observed SNe Ia, which typically have a rate of 1.5 mag $\times$ (100 d)$^{-1}$ (cf. Turatto et al. 1990; Suntzeff 1996).

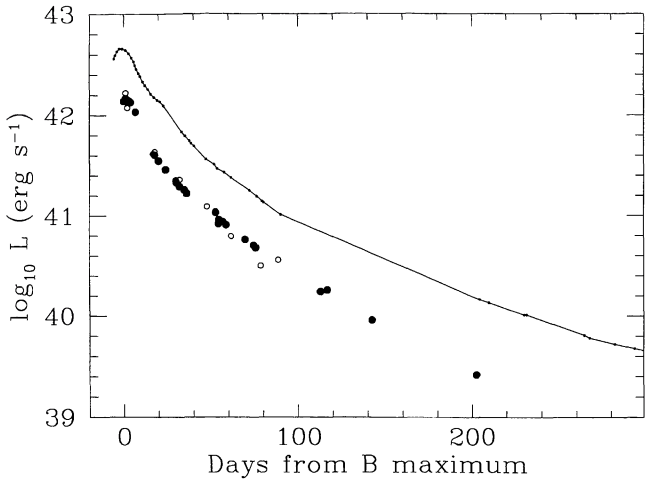

Figure 5. Bolometric light curves of SNe 1991bg (symbols) and 1992A (line). Filled symbols refer to *BVRI* photometry from this paper and from literature, while open symbols are derived from the flux-calibrated spectra of Table 2 with wide wavelength range. For the computation of the last point (day + 203) the *I* photometry has been linearly extrapolated from the previous epochs. For SN 1991bg we have used a bolometric correction of 0.1 dex constant with time (see text for a discussion of the relative luminosity), distance modulus 31.09 and reddening correction $E(B-V)=0.05$. The data for SN 1992A are from Suntzeff (1996).

mum was about three times fainter than the spectroscopically normal SN Ia SN 1992A ($\log L=42.65$) and, because of a faster luminosity decline, the difference increased to a factor 5 on day 200. It should be noted that, according to Suntzeff (1996), either the distance scale to SN 1992A is grossly in error, or this type Ia SN is underluminous with respect to the standard model, so the offset in peak $L_{\rm Bol}$ values in Fig. 5 does not indicate that SN 1991bg is a factor of 3 fainter than normal SNe Ia.

In Table 3 we present the main data of the bolometric light curve. The slopes have been determined making use only of the photometric determinations. It is evident from Fig. 5 that SN 1991bg was at all epochs steeper than SN 1992A which declined at a rate of 2.0 mag $\times$ (100 d)$^{-1}$ between days 72 and 210.

At the last epoch of observation (day 530) only the *V* magnitude is available, and thus no estimate of the bolometric luminosity is possible. We note, however, that assuming at this epoch the same spectral distribution as on day 203, the corresponding *uvoir* bolometric luminosity is about 10^{38} erg s^{-1}.

4 THE SPECTRAL EVOLUTION

The first available spectra of SN 1991bg were taken near maximum light. Fig. 6, which shows the spectra listed in Table 2, illustrates the overall spectroscopic evolution from the time of maximum to 7 months later.

4.1 The first two months

Although it showed the distinctive Si II absorption, the first available spectrum, taken at maximum appeared different from those for typical SNe Ia. In Fig. 7 the time evolution of the photospheric velocity deduced from Si II λ6355 is plotted. Clearly, the expansion velocity of SN 1991bg was quite low (at maximum, $v_{t=0}=9720$ km s^{-1}) and declined faster. Also, the blue wing of the Si II doublet, although possibly blended with another weak line, indicates a maximum expansion velocity for the Si II rich layers of only about 14500 km s^{-1}, to be compared with 16000 km s^{-1} of SN 1994D (Patat et al. 1996).

To highlight the peculiarities of SN 1991bg, in Fig. 8 the spectra of SN 1991bg at different epochs are compared to those of other SNe Ia at similar phases. Only SNe Ia with low expansion velocities have been selected. At maximum, the slope of the optical continuum differs from that of the normal SNe Ia 1994D and 1989B, once the latter is dereddened. Instead, it resembles the slope of SN 1986G (cf. top panel of Fig. 8) if one adopts for this SN a reddening $E(B-V)=0.6$ (Phillips 1993). Other similarities with SN 1986G can be seen, in particular in the broad absorption trough between 4200 and 4500 Å which has been noted early on (Benetti, Cappellaro & Turatto 1991). Filippenko et al. (1992) attributed this feature to Mg II 4481-Å and Ti II lines that could also account for a number of other features below 5000 Å, while Leibundgut et al. (1993) identified it with Fe III. The spectrum synthesis analysis (Mazzali et al. 1996) supports the Ti II identification.

As in SN 1986G, the red wing of the Si II λ6355-Å absorption seems to be contaminated by another absorption line. After deblending, the latter was measured at about 6255 Å in the parent galaxy rest frame. Leibundgut et al. (1993) have proposed C II λ6580 Å or Hα from hyrogen expanding at velocities of the order of 14000 km s^{-1} as possible identifications. The similarity with SN 1986G extends to the absorption at about 5800 Å attributed to Si II λ5968, which in both SNe is stronger than in normal SNe Ia. Also, the two lines of S II near 5500 Å have similar intensity, while the redder one is usually stronger in other SNe Ia at this epoch.

As in other SNe Ia spectra, in the near-IR the strong P Cygni profile of the Ca II triplet is possibly contaminated by O I λ8446. The absorptions at 7600 Å, owing to O I λ7772–7775 and Mg II λ7877–7896, and that at 8900 Å owing to Mg II λ9217–9243, are instead much stronger than usual.

There is a 2 week gap in the temporal coverage both in our spectroscopic observations and in those of Filippenko et al. (1992) and Leibundgut et al. (1993). When the SN was observed again at the end of December, about 2 weeks after maximum, the spectrum was quite different (cf. Fig. 6). At this point the rapid post-maximum decline phase is over, and the SN enters what, in Section 3, we called the *intermediate* phase of the light curve. The continuum is now redder (cf. also Fig. 4) and emission lines, which are commonly observed in SNe Ia only at later epochs, start to appear. The λ6355 Si II absorption is still present, while the corresponding emission has strengthened and has moved redward. [Ni III] λ6536 may also contribute to this emission. On the other hand, the Si II absorption at 5810 Å (5792 Å in the galaxy rest frame) disappeared, probably as a result of the drop in temperature lowering the population of the lower level which is 2 eV higher than the corresponding level giving the Si II 6355 line. The Ca II IR lines are very strong and the lines of O I and Mg II have decreased their

al. (1995) for their *ridge-line* SNe Ia, i.e. SNe Ia that suffered little extinction. SN 1991bg is even more extreme compared to the average SNe Ia magnitudes derived with the Cepheid distance calibration ($M_B = -19.65 \pm 0.13$ and $M_V = -19.60 \pm 0.11$: Saha et al. 1995).

At present, it is widely accepted that some degree of heterogeneity is present within the class of SNe Ia (e.g. Hamuy et al. 1995; Patat et al. 1996). This may be partially described by a relation between the peak luminosity and the initial decline rate (Pskovskii 1967; Phillips 1993; Hamuy et al. 1995). However, even in this context the low luminosity of SN 1991bg is exceptional, since this SN does not lie on the extension of the peak luminosity–decline rate relation observed for the slowly declining objects (Hamuy et al. 1995).

3.3 Colour curves

The evolution in three different colours is shown in Figure 4, in which the comparison is made with the well-studied SN 1994D which had comparable reddening to 1991bg and whose colour evolution was similar to 1992A (Patat et al. 1996).

The two SNe show significantly different colour evolutions. At maximum, SN 1991bg had $(B-V) \sim 0.75$, i.e. it was ~ 0.8 mag redder than SN 1994D. Were the colour differences due to reddening for SN 1991bg, which we excluded (cf. Section 3.2), this would indicate $A_B = 3.2$ yielding $M_B = -19.54$. With such values SN 1991bg would be the brightest SN Ia in the samples studied by Vaughan et al. (1995) and Phillips (1993). At the time of maximum, SN 1994D was still evolving to the blue, with minima in $(V-R)$ and $(V-I)$ corresponding to the minima between the two peaks of the R and I light curves (Patat et al. 1996). On the contrary, SN 1991bg at the same epoch was already rapidly evolving to the red. SN 1991bg reached the reddest colours [$(B-V) = 1.45$, $(V-R) = 0.60$ and $(V-I) = 1.25$] at about $t = 15$–17 d, corresponding to the first bending point of the B light curve, while in SN 1994D the maxima of the colours were reached somewhat later ($t = 25$ d) at $(B-V) = 1.05$, $(V-R) = 0.37$ and $(V-I) = 0.65$. Diversity in the colour evolution of SNe Ia (especially in proximity of the maximum) have been noted by Maza et al. (1994) and Patat et al. (1996) but, to our knowledge, no other object appears as odd as SN 1991bg.

After the colour maxima, SN 1991bg turned to the blue and starting at about day 40–50 it matched the $(B-V)$ and $(V-R)$ curves of normal SNe Ia (Fig. 4). The $(V-I)$ curve, instead, never conformed with that of 1994D, remaining always considerably redder. This gives us an indication that the late overall light distribution of SN 1991bg is similar to normal SNe Ia but for a flux excess in the I band. In Section 4.2 this is ascribed to the unusually strong [Ca II] emission lines.

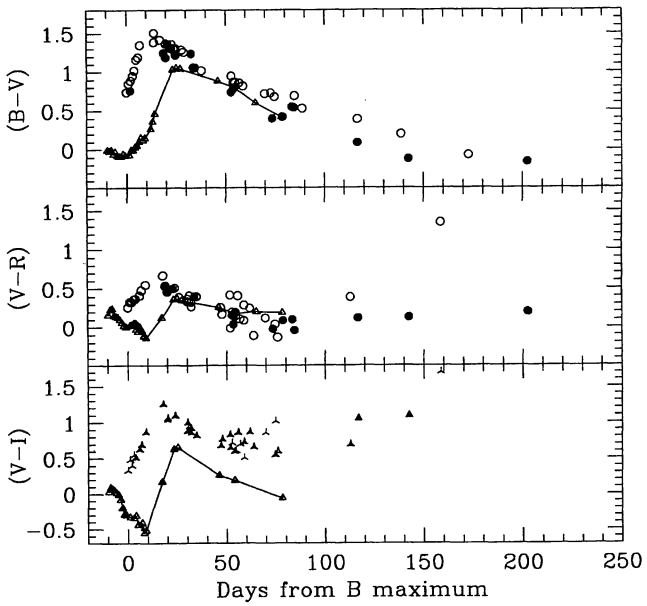

Figure 4. The colour curves of SN 1991bg compared to those of SN 1994D (connected by solid lines) which has a reddening similar to SN 1991bg (Patat et al. 1996). Filled symbols are observations from Table 1, open symbols are data from literature. Note the scatter at late epochs.

3.4 The bolometric light curve

The optical light curves of SN 1991bg are well defined in four bands for several months. These allowed us to estimate the *uvoir* bolometric luminosity by applying reasonable corrections to the optical data. Suntzeff (1996) showed that in normal SNe Ia at early phases the flux below 4000 Å is less than 40 per cent of the total flux and rapidly declines to below 10 per cent already at 80 d after maximum. Also the contribution of the IR above 9000 Å is always low (less than 15 per cent, Suntzeff 1995). In the case of SN 1991bg the dominance of the *BVRI* bands is even larger: merging the (single) UV spectrum, taken with the *IUE* satellite at B maximum (Cappellaro, Turatto & Fernley 1995), with our nearly simultaneous optical observations, we have estimated that the flux below 4000 Å is only ~ 10 per cent of the total flux in the range 1900–9000 Å. Also the *JHK* infrared observations of SN 1991bg (Porter et al. 1992) indicate a low luminosity at maximum followed by a rapid decline of 3 mag in the first month, with no sign of a secondary maximum. It is reasonable to assume that in SN 1991bg the UV contribution decreased with epoch while the near-infrared one increased up to 15 per cent of the total *uvoir* flux analogous to SN 1992A (Suntzeff 1996). This means that at all epochs about 80 per cent of the total flux of SN 1991bg is emitted in the *BVRI* domain, corresponding to a constant correction of 0.10 dex. Spectral modelling, discussed by Mazzali et al. (1996), gives results in good agreement with this assumption.

The evolution of the bolometric luminosity is compared in Fig. 5 to that of SN 1992A (Suntzeff 1996). Both *BVRI* photometry (from this paper and literature) and spectrophotometric data have been used. A distance modulus of 31.09 and a reddening correction $E(B-V) = 0.05$ have been adopted (cf. Section 3.2).[1] Thus SN 1991bg at maxi-

[1]The maximum bolometric luminosity of SN 1991bg, $\log^{10} L = 42.20$, is about 0.25 dex (i.e. a factor of 1.8 in luminosity) fainter than in fig. 7 of Suntzeff (1996) who adopted a similar distance modulus and no reddening correction. The inconsistency is probably due to a different correction factor.

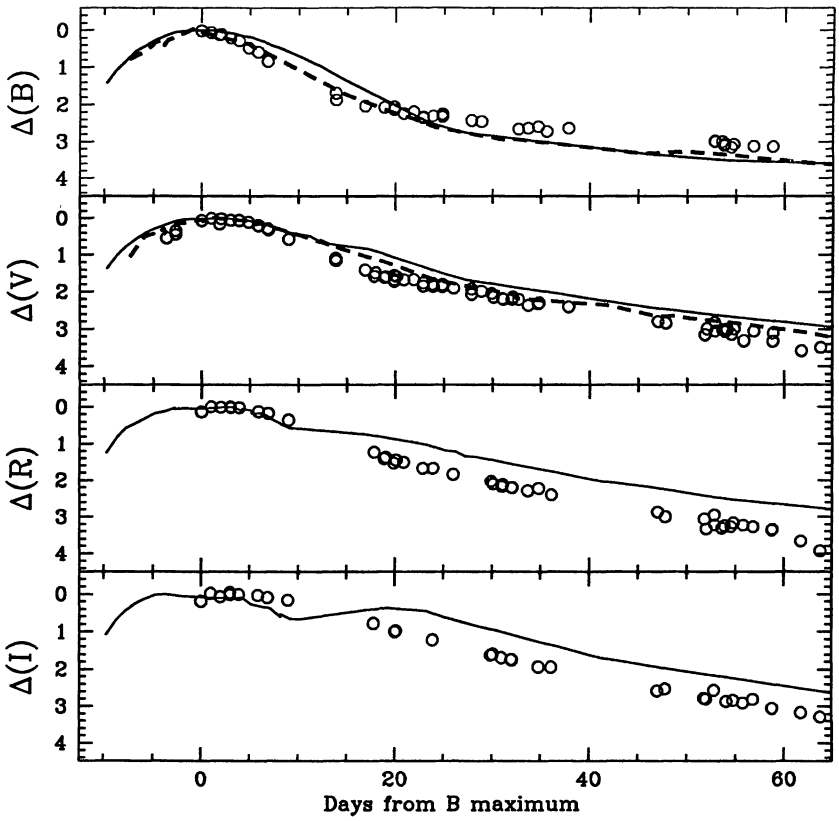

Figure 3. Comparison between the early light curves of SN 1991bg (open circles), SN 1994D (solid lines, Patat et al. 1996) and SN 1986G (short-dashed lines, Cristiani et al. 1992). In the four panels, zero in the abscissa corresponds to the epoch of the *B* maximum while in the ordinates it is the magnitude at maximum in the specific photometric band.

Finally, the observation of 530 d after maximum indicates that after day 200 the luminosity decline was significantly lower, 1.2 mag $\times$ (100 d)$^{-1}$ based only on the two last observations. Owing to the 300-d gap in the observations, it is impossible to determine if the change was gradual or if a new bending point characterizes the late light curve. We note, however, that the observed decline rate is still steeper than that of ^{56}Co to ^{56}Fe decay [0.98 mag $\times$ (100 d)$^{-1}$].

3.2 The absolute magnitude at maximum

NGC 4374, the parent galaxy of SN 1991bg, lies in the core of the Virgo cluster. This makes it possible to compare directly the apparent magnitude of SN 1991bg with that of other SNe Ia in the cluster. A list of the Virgo SNe Ia with 'normal' spectra and reliable photometry was given by Patat et al. (1996) (their table 4): the average apparent magnitude is $B_{max} = 12.22 \pm 0.44$, to be compared with $B_{max} \sim 14.75$ for SN 1991bg. Two other SNe Ia have been discovered in NGC 4374, SN 1957B and 1980I (cf. Turatto, Cappellaro & Benetti 1994). Both SNe show apparent magnitudes in agreement with that of normal SNe Ia in Virgo. Therefore, if no significant reddening was present, SN 1991bg was, at maximum, 2.5 mag fainter in the *B* band than normal SNe Ia.

Strong reddening is not expected, since the parent galaxy is elliptical. Actually a dust lane, elongated in the east–west direction, crosses the galaxy nucleus (cf. Filippenko et al. 1992; Leibundgut et al. 1993) but the SN is located about 1 arcmin to the south of the nucleus and hence no significant contamination is expected. In fact, a careful examination of our best S/N spectra (cf. Section 4) did not show signs of narrow interstellar Na I D at the expected position (5913 Å). In a few spectra a weak absorption feature might be present at about 5890 Å that may be a result of interstellar Na I D within the Galaxy ($A_B = 0.13$: Burstein & Heiles 1984). Indirect, but independent, support for low reddening comes from the spectral modelling at early and late epochs by Mazzali et al. (1996). Those models require low photospheric temperatures. This, together with the fact that all three colours, $B-V$, $V-I$, $V-R$ are redder than normal SNe Ia immediately after maximum but return to normal colours 30 d past maximum, suggests that neither internal dust formation nor line-blanketing owing to additional abnormally strong lines are the cause of the red colours. In agreement with other papers on this SNe, we will adopt in the following $E(B-V) \sim 0.05 \pm 0.02$ as the total reddening suffered by SN 1991bg. Given the low reddening, it is clear that SN 1991bg was *intrinsically* faint and red.

For homogeneity with Patat et al. (1996) and Vaughan et al. (1995) who studied large samples of SNe Ia, we adopt for NGC 4374 the distance derived using the SBF method ($\mu = 31.09 \pm 0.30$: Ciardullo, Jacoby & Tonry 1993). Taking into account the (small) reddening, we obtain for SN 1991bg the following absolute magnitudes: $M_B = -16.54 \pm 0.32$, $M_V = -17.28 \pm 0.31$, $M_R = -17.58 \pm 0.31$ and $M_I = -17.68 \pm 0.31$. These values are significantly fainter and redder than the mean, $M_B = -18.64 \pm 0.05 + 5\log(H_0/85)$ and $M_V = -18.63 \pm 0.06 + 5\log(H_0/85)$, found by Vaughan et

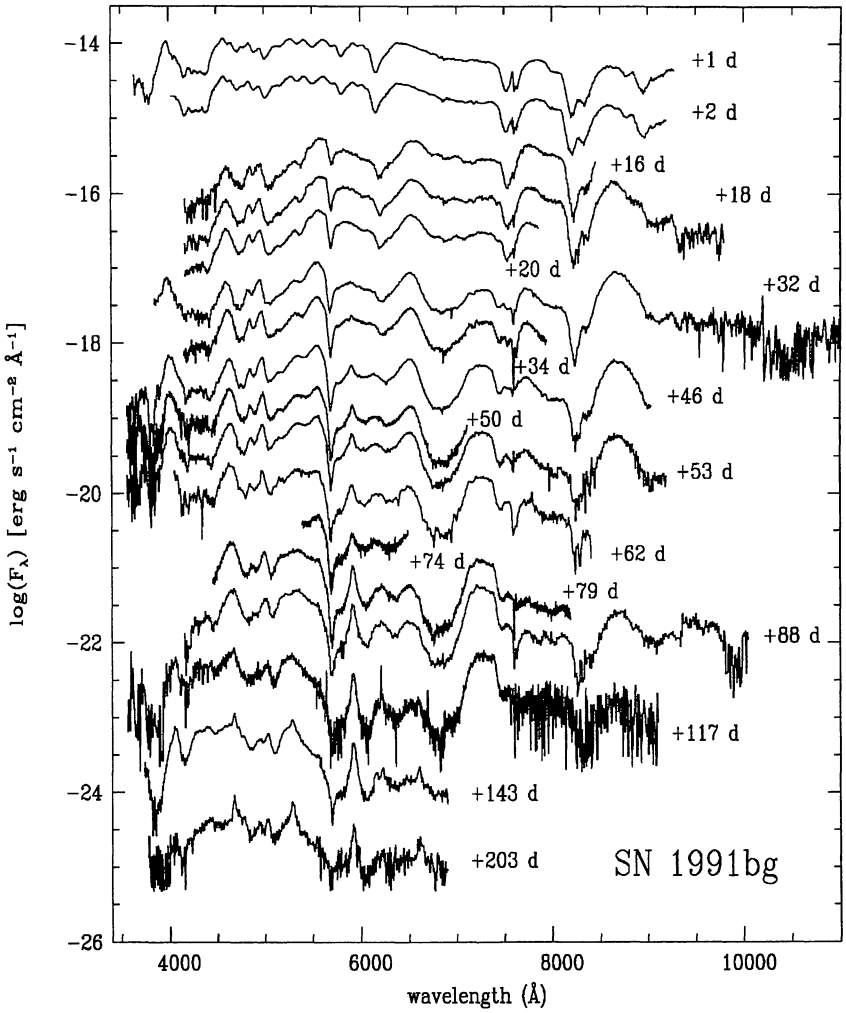

Figure 6. The spectral evolution of SN 1991bg from day +1 to +203. The ordinate refers to the first spectrum ($t = +1$ d); all other spectra are shifted downwards by 0.45 dex with respect to the one above, with the exception of the last three, for which the shift is 0.65 dex.

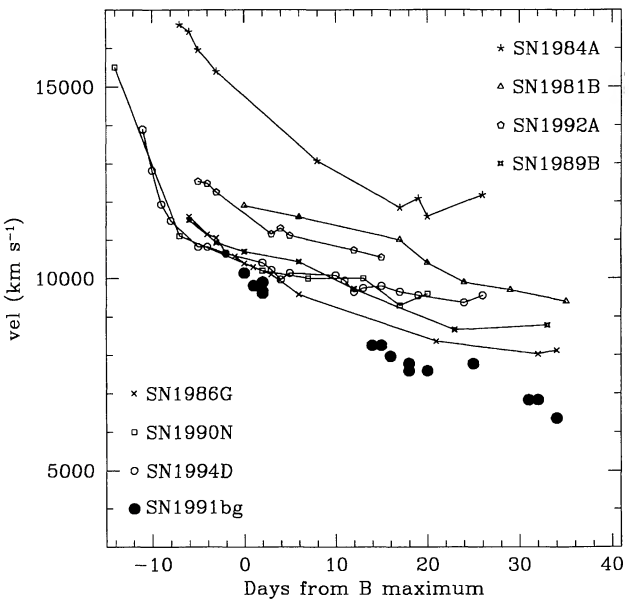

Figure 7. Expansion velocities of SNe Ia as as deduced from the minimum of the Si II λ6355 line. Data of SN 1991bg are from this paper and Leibundgut et al. (1993).

intensities. Now the Ca emission dominates over the absorption.

The strong and relatively narrow absorption feature, measured on day 18 at about 5705 Å (5687 Å in the galaxy rest frame[2]), is quite unusual. This line, which was also barely visible in the spectra at maximum, will persist for about 5 months. The line profile is strongly asymmetric but definitely narrower than all other absorption features in the spectrum, FWHM $\sim$2500 km s^{-1}, and constant with time. If the feature is attributed to Na I D (Filippenko et al. 1992), the expansion velocity of the absorbing layer, $v_{\rm Na\,II} = 10\,500$ km s^{-1}, is much larger than that of Si II ($v_{\rm Si\,II} = 7600$ km s^{-1}) at this epoch. Leibundgut et al. (1993) attributed this feature at early epochs to a blend of Si II lines, but its narrowness with respect to other Si II lines and its persistence after Si II 6355 has faded makes this doubtful. An unlikely identification is He I λ5876 expanding at about 9600 km s^{-1}, because of the low photospheric temperature, unless non-thermal excitation of appropriate levels is effective. We lack independent evidence of non-thermal effects. In any of these cases, however, the high expansion velocity and the

[2]Throughout this paper we have adopted for SN 1991bg the recession velocity of NGC 4374, $v = 933$ km s^{-1} (Tully 1988).

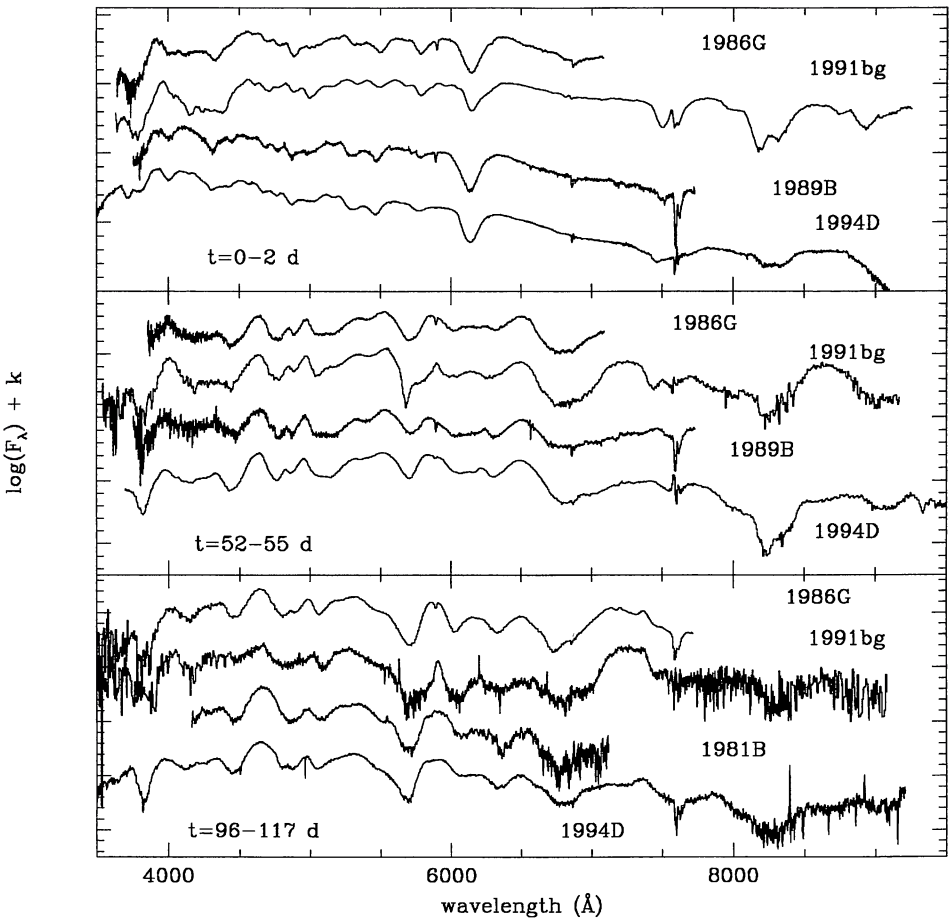

Figure 8. Comparison of the spectra of SN 1991bg at maximum (top panel), around 50 (middle) and 100 (lower) d past maximum with those of other SNe Ia: the 'normal' SNe 1194D and 1981B, 1989B and the peculiar SN 1986G. The spectra of SN 1986G and SN 1989B have been dereddened by $E(B-V)=0.6$ and 0.35, respectively (Phillips 1993). The tracings have been displaced by arbitrary units and reported to the rest frames of the parent galaxies. References are Cristiani et al. (1992) for SN 1986G; Barbon et al. (1990) for SN 1989B; Patat et al. (1996) for SN 1994D (early times); Branch (1984) for SN 1981B.

narrow width confine the ion from which the line forms to a relatively thin outer layer. This would then be clear-cut evidence of stratification in SN Ia ejecta.

However, the feature changes very little in velocity over the 200 d of observation, in contrast with other absorption features.

The line drifts from 5710 Å on day 1 to 5700 Å at about 50 d past maximum, in good agreement with the measurements of Leibundgut (1993). Thus the correct interpretation may have to await a detailed modelling to ascertain whether radiation transfer effects which describe the redward progression of photons in the expanding photosphere can produce this feature.

On day 50 all absorptions (5700-Å feature excepted) have drifted notably to the red with respect to the initial position, indicating that the photospheric expansion velocity has decreased significantly. The Ca II lines appear at early phases stronger in absorption than in other SN Ia, in particular the IR triplet; and stronger in emission at later phases, in particular [Ca II] λ7291–7324. Although abundance effects may play a role, a temperature effect must be important. Apart from this peculiarity, overall the spectrum at this phase resembles that of normal SN Ia.

4.2 The nebular phase

For the first time on day 34 we detect a relatively narrow emission line redward of the absorption at 5700 Å, at about 5915 Å (rest wavelength, 5897 Å; cf. Fig. 6). From this epoch on, and up to our last observation, the relative intensity of this emission keeps increasing. The line profile, with a narrow core, shows very small or negligible velocity evolution redwards. Because of the rest wavelength, the line was identified with the Na I D line (Filippenko et al. 1992; Ruiz-Lapuente et al. 1993), but in the light of the results of Mazzali et al. (1996) we propose an alternative identification with [Co III] λ5890–5908, although a contribution from Na I D, especially at early phases, cannot be ruled out.

The spectral evolution continues with the progressive decrease of the continuum and the relative increase of the emission lines. The absorptions fade, with the exception of the narrow feature at λ5700. With the third month the SN enters the late decline phase of the light curve (cf. Section 3). Corresponding to this transition, the emission line of [Co III] drifts by about 10 Å redwards, as measured by Leibundgut et al. (1993).

On day 117 the dominant feature is the [Ca II] line at

7150–7400 Å (cf. Fig. 8, bottom panel) which, as we mentioned, is much stronger than in other SNe Ia at a comparable epoch, while the blue part of the spectrum shows the features typical of other SNe Ia, although they are significantly narrower. Also, the emissions at 4680 and 5290 Å increase in relative strength as the SN ages.

The last available spectrum of SN 1991bg was obtained on 1992 July 3 (day 203). All lines present on days 117 and 143 are visible and correspond to the typical emission lines in the spectra of SNe Ia at this epoch (Fig. 9). In particular, the bulk of the emission is between 3800 and 5700 Å, with strong peaks at about 4400, 4700, 5000 and 5300 Å. All lines appear to be significantly narrower than in other SNe Ia, confirming the indication that the expansion velocity in SN 1991bg was smaller than in typical SNe Ia.

We note that our observations are in contradiction to those of Ruiz-Lapuente et al. (1993). While their 1992 May 24 spectrum resembles our spectrum of May 4, their last spectrum (June 29) taken at the WHT appears remarkably different from our spectra taken only 4 d later. In particular, their spectrum does not show the strong emission features between 4500 and 5500 Å, and is completely different from those of normal SNe Ia.

A late-time spectrum of SN 1991bg, obtained at the same epoch and with the same telescope, was shown by Gomez & Lopez (1995). Although the authors do not state so, this is probably a new reduction of the WHT observation reported by Ruiz-Lapuente et al. (1993). Puzzling enough, the two tracings do not show the same features. In particular, the narrow emissions seen in Ruiz-Lapuente et al. (1993) near 5900 and 6570 Å are absent in the Gomez & Lopez (1995) spectrum, which does not reach wavelengths bluer than 4600 Å. Nevertheless this spectrum too is definitely different from ours.

The most likely explanation for the disagreement between our spectrum and those shown by Ruiz-Lapuente et al. (1993) and Gomez & Lopez (1995) is their inaccurate positioning of the slit on the target and/or a non-alignment of the slit with the parallactic angle. In our case, exploiting the multimode capability of EFOSC, the slit was accurately positioned based on the previous imaging of the field in the *B* band. An independent confirmation of our spectroscopic calibration is obtained from the $(B-V)$ colour curve (Fig. 4), which indicates blue colours for the SN at late epochs.

In Table 4 we list the rest-frame positions of the narrow lines marked in the late-time spectrum of Fig. 9. Typical errors are ± 1 Å, but for the features of poorer signal-to-noise ratio the errors can be as large as ± 5 Å. Line identifications are based on the non-local thermodynamic equilibrium (NLTE) synthetic nebular spectra presented by Mazzali et al. (1996), which reflect the earlier results of Meyerott (1980). The identification of the λ5906 line with [Co III] is supported both by the line position and by the relative ratio of the flux with the [Fe III] line at about 4700 Å. In fact, according to Kuchner et al. (1994) the time evolution of the Fe/Co flux ratio supports the idea that the Ni–Co–Fe chain powers SNe Ia. The value of this ratio in our nebular spectra are $R=2.5$, 3.0, 4.1 and 4.2 (with errors of the order of 20 per cent) on days 88, 117, 143 and 203, respectively. These values are consistent with those of other SNe Ia and with the Ni decay model for the origin of Co and Ni also in this SN.

All the other emission features marked in Fig. 9 find satisfactory identifications with forbidden lines of Fe-group elements, with the exception of the feature labelled *K*, which, in our spectra is measured at about λ6590 Å (rest wavelength) with a FWHM ~ 2000 km s^{-1}, similar to that of the [Co III] λ5890–5908 line. This line is present on all spectra from day 79 onwards, and is also visible in the spectra by Leibundgut et al. (1993) starting at about the same epoch. The line was present in the spectrum of Ruiz-Lapuente et al. (1993) but was measured at λ6570 and

Table 4. Emission in the nebular spectra of SN 191bg.

desig.	ident.	rest frame position (Å)			
	epoch:	+88 d	+117 d	+143 d	+203 d
A	[FeIII] 4658-4702		4665	4668	4670
B	[FeIII] 4733			4716	4714
C	[FeIII] 4755-4769-4778			4765	4767
D	[FeIII] 4931		4925	4928	4935
E	[FeIII] 5011		5014	5027	5019
F	[FeII] 5261-5273, [FeIII] 5270		5274	5280	5284
G	[FeII] 5527	5542	5540	5536	5529
H	[CoIII] 5890-5908	5906	5907	5908	5906
I	[CoIII] 6129	6144:		6142	6157
J	[CoIII] 6197	6204	6211	6212	6211
K	[CoIII] 6578, Hα ?	6584	6586	6592	6595

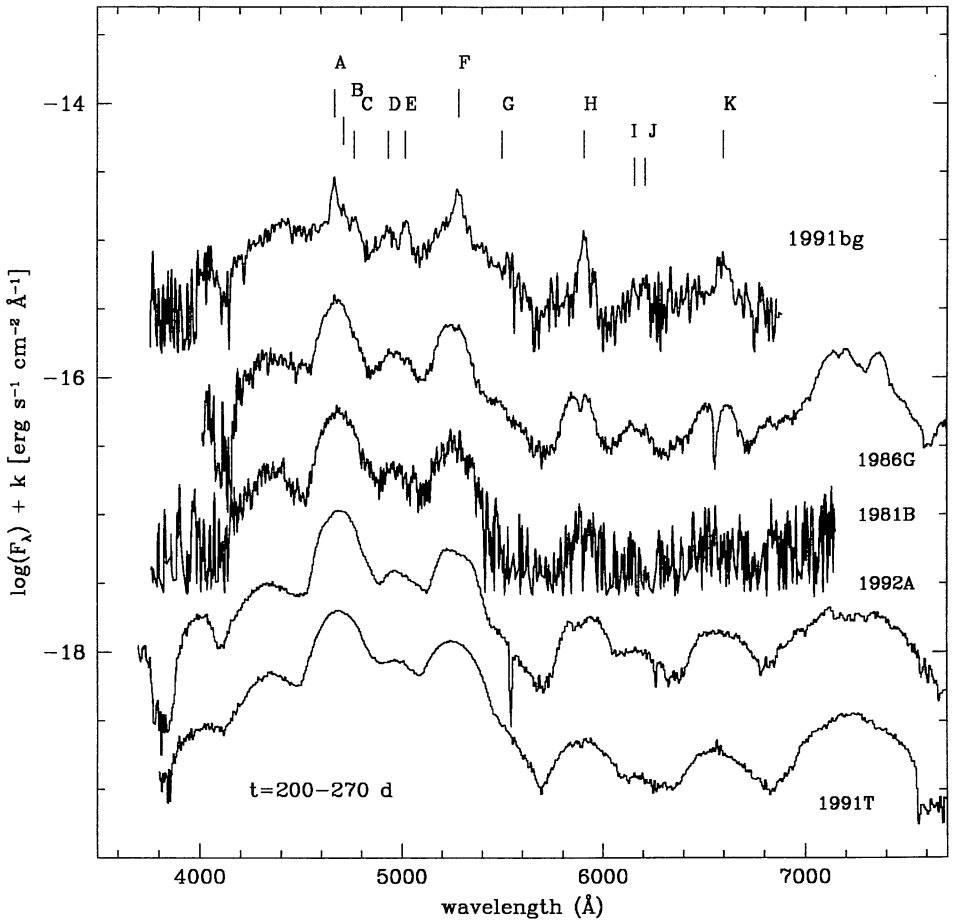

Figure 9. Comparison of the last spectrum of SN 1991bg (203 d past maximum) with those of other SNe Ia at similar epochs: the normal SNe 1981B and 1992A, the peculiar SNe 1986G and 1991T. The spectrum of SN 1986G has been dereddened as in Fig. 8. The narrow emission lines are marked according to Table 4. The spectra have been displaced by arbitrary units and reported to the rest frames of the parent galaxies. The spectra of SNe 1981B and 1986G have the same sources as in Fig. 8; the spectrum of SN 1992A was obtained on 1992 September 2 at the 3.6-m telescope equipped with EFOSC; the same equipment was used on 1992 February 5 for SN 1991T.

identified with Hα. In their proposed scenario, the Hα emission comes from hydrogen stripped from an extended, hydrogen-rich companion star as a consequence of the explosion, and it remains at low velocity. Given our measurement of the redshift of this feature of 1200 km s^{-1} with respect to the rest wavelength of Hα, we can exclude the possibility that the line is a result of Hα emission from hydrogen surrounding the exploding star. However, we cannot rule out the possibility that the line arises from hydrogen stripped from a companion which at the moment of the explosion was on the far side of the SN with respect to the observer. In this case, high-velocity hydrogen blobs mixed with the expanding material might emit redshifted lines. However, since an emission line is present at this wavelength in the nebular spectra of all SNe Ia (cf. Fig. 9), and with a width comparable to that of all other spectral features, if this line is attributed to hydrogen in SN 1991bg a similar identification should be invoked for all other SNe Ia together with the implication that this hydrogen is situated in the expanding envelope. We note that the possibility of interpreting this line as Hα was mentioned by Cristiani et al. (1992) for SN 1986G. Another possible identification is with [Co III] λ6578, while lines of Fe II and [Fe II] also fall in this region of the spectrum. Without modelling the identification with [Co III] is not easy to understand, since it appears to increase in strength relative to the proposed [Co III] 5890–5908 line. It should be further noted that this feature is slightly redshifted in SN 1991bg relative to the broader feature in other supernovae, while there is no significant redward displacement of other emission features at shorter wavelengths. Whether or not this points to a different identification in this supernova from that in others awaits clarification.

5 ARE THERE RELATIVES OF SN 1991bg?

In recent years a number of SNe have been indicated as possible relatives (ranging from 'twins' to 'close cousins') of SN 1991bg.

We have already mentioned that SN 1986G was found to share some of the properties of SN 1991bg (cf. Sections 3.1 and 4), in particular the peculiar broad absorption between 4200 and 4500 Å. Also, the early light curve decline was fast but the duration and the slopes of the various portions of the light curve were different (Leibundgut et al. 1993) and so was the $(B-V)$ colour evolution. The absolute magni-

tude of SN 1986G may have been similar to that of a normal SNe Ia, but because of the conflicting evidence on the reddening for SN 1986G (cf. Section 5 of Filippenko et al. 1992) no conclusive statement can be made. The late-time spectra of SN 1986G showed relatively strong [Ca II] lines, similar to SN 1991bg (cf. Fig. 8, bottom panel), and also the lines were somewhat narrower than in normal SNe Ia (cf. Table 5) but still broader than in SN 1991bg. It appears, therefore, that while the chemical composition and the physical conditions of the outer layers were rather similar in the two SNe, both showing red continua with Ti II lines, at least the kinematics of the inner layers were different.

Filippenko et al. (1992) suggested that SN 1971I is another possible relative of SN 1991bg. Inspection of the light curve shows that this SN, although it faded relatively fast [12.6 mag × (100 d)$^{-1}$ in B], maintained a close resemblance to typical SNe Ia until day 300. Moreover, the 4200–4500 Å absorption band is absent in the spectra taken at maximum (Kikuchi 1971; Barbon et al. 1973b) and the Si II line indicates a normal expansion velocity (about 11 600 km s^{-1} a couple of days before maximum).

In a recent paper by Hamuy et al. (1994) it has been proposed that SN 1992K in ESO 269-G57 is a twin of SN 1991bg. This SN has broad absorption between 4200 and 4500 Å, a somewhat slow expansion velocity, an intrinsic red continuum and a low luminosity. In Fig. 10 we show the comparison of a spectrum of SN 1992K taken at La Silla on 1992 April 7, with those of SNe 1991bg and 1986G at a similar age. The three spectra are rather similar, both in the blue, with the 4200–4500 Å trough, and in the near-IR, with the presence of strong Ca IR triplet and [Ca II] λλ7291, 7324. In SN 1992K, however, the features at 5700 and 5900 Å are broader and similar to SN 1986G.

Although SN 1992K was not observed at maximum, the comparison of the light curves with those of five different templates of SNe Ia has shown that SN 1992K was indeed very similar to SN 1991bg (Hamuy et al. 1994). In particular, between days 70 and 150, SN 1992K had a decline rate, $\gamma_V = 2.75$ mag × (100 d)$^{-1}$, which is identical to that of SN 1991bg (cf. Table 3). Based on this similarity it was possible to estimate that the maximum of SN 1992K occurred probably on 1992 February 5 at an absolute magnitude $M_B = -16.84$, slightly brighter (0.4 mag) than 1991bg but still fainter than normal SNe Ia (we note that also for SN 1992K there is no evidence of significant reddening).

Another SN that has been proposed for inclusion in the SN 1991bg family is SN 1991F in NGC 3458 (Gomez & Lopez 1995). This SN was observed only spectroscopically at epochs estimated between 3 and 5 months past maximum. Similar to SN 1991bg at the same epoch, the spectrum of SN 1991F is dominated by emission lines which are narrower than in normal SNe Ia, indicating a lower expansion velocity; and it shows strong Ca II lines. The presence, in the spectrum taken 80–90 d past maximum, of two very narrow features in absorption at λ5700 and in emission at λ5900, with profiles very similar to those of the corresponding features in SN 1991bg, is of interest. However, the position of the emission in SN 1991bg (Table 4) is about 20–30 Å redder than in SN 1991F (table 2 of Gomez & Lopez 1995) at the same epochs, and, unlike SN 1991bg, the λ5700 absorption in SN 1991F weakens with age. Moreover, the [Fe II] + [Fe III] emission at about 5200 Å is still weak at $t = +144$ d, while in SN 1991bg at the same epoch it is prominent. Rough estimates based on spectrophotometry (Gomez & Lopez 1995) seem to indicate that the late-time luminosity and the decline rate of SN 1991F are comparable to those of SN 1991bg.

In summary, it appears that there are at least three SNe Ia (namely SNe 1986G, 1991F and 1992K) that share some of the peculiar characteristics of SN 1991bg, in particular the low luminosity, fast fading rate, red colour at maximum, low expansion velocities, evidence of Ti II lines in the photospheric spectrum, strong Ca II and narrow emission lines at late epochs. However, none of these SNe displayed all these features simultaneously and with such strengths as SN 1991bg.

The relative frequency of objects such as SN 1991bg is difficult to estimate. Because SN searches are magnitude limited, the discovery probability of intrinsically faint SNe Ia is lower than that of normal SNe Ia. Therefore, the fraction of faint SNe Ia so far discovered (about 5 per cent) must be considered as a lower limit of the true value. On the other hand, the relative rate of faint SNe Ia can be estimated based on the few observed events by using the control time method if the details of individual SN searches were known. At present this kind of data is available only for the Asiago + Crimea SN search (Cappellaro et al. 1993). From this data base we estimate that faint (1991bg-like) SNe Ia are at most 40 per cent of all SNe Ia, hence the real number should be between 5 and 40 per cent.

Table 5. Expansion velocities versus absolute magnitude for SNe Ia.

SN	M_V^{max}	$\Delta m_{15}(B)$	v(SiII)[a] [km s^{-1}]	FWHM([CoIII])[b] [km s^{-1}][day]
1991bg	-17.28	1.95	9800	2340 [203]
1986G	-18.22[c]	1.73	10400	7120 [256]
1981B	-18.50	1.10	11900	8140: [270]
1992A	-18.00	1.33	11700	10170 [227]
1991T	-19.51[d]	0.94	9800[e]	11190 [262]

(a) Photospheric velocity at B maximum as measured from the Si II λ6355 absorption; (b) full width half maximum of [Co III] λλ5890–5908 emission at epochs between 200 and 270 d (indicated in brackets); (c) $E(B-V) = 0.6$ (Phillips 1993); (d) $E(B-V) = 0.13$ (Phillips et al. 1992); (e) the expansion velocity of Si II in SN 1991T was a poor indicator of the photospheric velocity. Velocities measured from other lines were significantly larger than in normal SNe Ia (Phillips et al. 1992).

6 DISCUSSION

According to the commonly accepted classification criteria, SN 1991bg was certainly of type Ia. The early spectrum shows most of the typical SNe Ia features due to intermediate mass elements, in particular the strong Si II λ6355 absorption (Fig. 8), although with noticeable differences in the relative line intensities. This implies that the physical

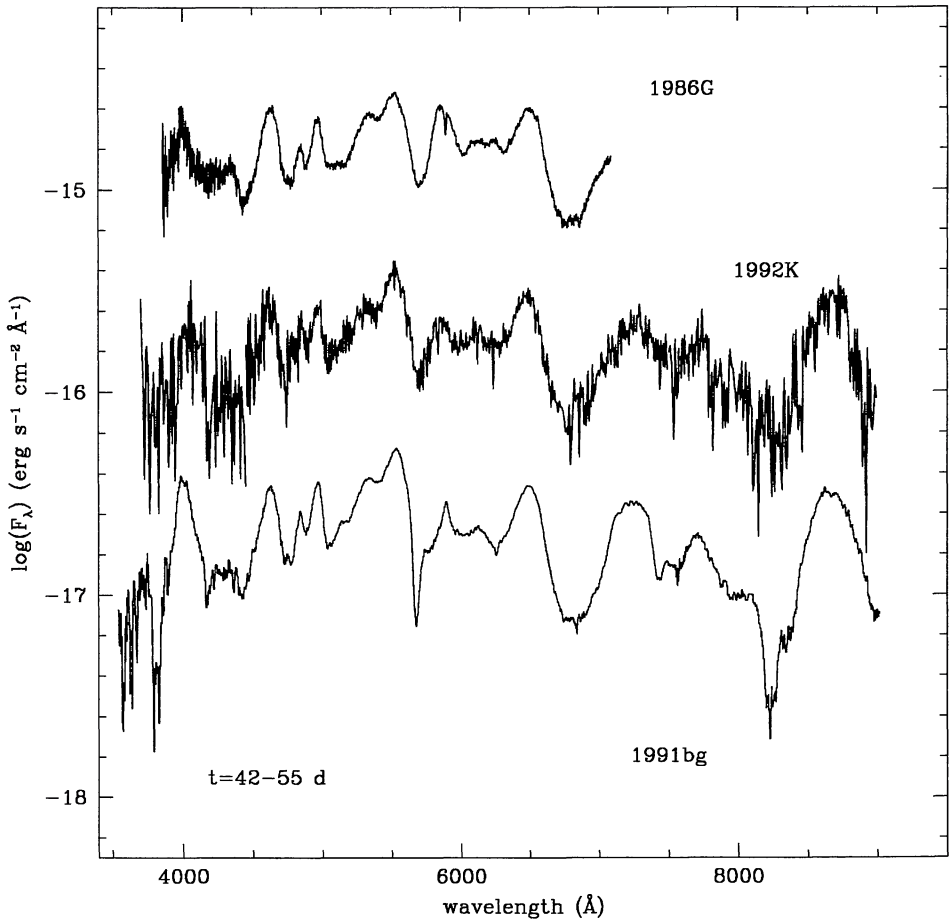

Figure 10. Comparison of the spectrum of SN 1992K taken on 1992 April 7 at the 2.2-m telescope (with EFOSC2 and grisms 1, 5 and 6) and corresponding to an epoch $t = +42$ d (1991bg templates), with those of SN 1991bg on day $+46$ and SN 1986G on day $+55$ (Cristiani et al. 1992). The spectrum of SN 1986G has been dereddened as in Figs 8 and 9. The ordinates are relative to the spectrum of SN 1992K, while the other two have been shifted by arbitrary units for easier comparison. In abscissa are the rest-frame wavelengths.

conditions in the near-photospheric layers around maximum light and the outer layers of the exploding star were not dramatically different from the usual ones.

Contrary to previous claims, we have shown in Section 4.2 that also in the nebular spectra of SN 1991bg, in particular in the latest observation at $t = 203$ d (Fig. 9), the relative intensities of the emissions match those of normal SNe Ia. Since at late epochs the line-forming region is deep inside the ejecta, this indicates that the composition as well as the physical conditions of the interior (temperature, density, ionization, etc.) are similar too. However, the lines are significantly narrower, hence the expansion velocity of the ejecta must be smaller. The luminosity at maximum ($M_B = -16.54$) is about 2.5 mag fainter than normal SNe Ia (cf. Section 3.2) while the bolometric luminosity is about 0.5 dex fainter than SN 1992A.

It is believed that the light curve of SNe is powered by the radioactive decay chain ^{56}Ni–^{56}Co–^{56}Fe and that, to a first approximation, the peak (bolometric) luminosity is equal to the instantaneous emission of the radioactive decay (Arnett, Branch & Wheeler 1985). As a consequence there is a direct relation between the mass of synthesized ^{56}Ni and the luminosity of the SN: since most SNe Ia show only a small scatter in absolute magnitude, this implies that most SNe Ia produce similar amounts of radioactive Ni. At present, explosion models suggest that normal SNe Ia produce 0.6 $M_\odot$ of Ni (e.g. Nomoto, Thielemann & Yokoi 1984).

Therefore, if we accept that a normal SNe Ia produces approximately 0.6 $M_\odot$ of Ni and, from the discussion above, that SN 1991bg had a bolometric luminosity 0.5 dex fainter than SN 1992A, we conclude that SN 1991bg produced < 0.2 $M_\odot$ of Ni (in Section 3.4 we noted that SN 1992A might be fainter than normal SNe Ia). This mass could conceivably be lower still depending on the nature of the explosion and, of course, on whether SN 1992A produced a smaller mass of Ni. For example Höflich, Khokhlov & Wheeler (1995) have demonstrated with a sample of different explosion models that the factor involved in relating bolometric luminosity at maximum to the γ-ray luminosity and hence to mass of Ni could vary by as much as approximately 50 per cent. A slightly larger difference in bolometric luminosity between the above two SNe is apparent at 100 d. However, an added complication in making a comparative quantitative estimate of Ni mass is the as yet unknown possible difference in γ-ray opacity of the two envelopes also at these later phases.

The mass of ^{56}Ni has been used as an input parameter also in the computation of the late-time synthetic spectra by

Mazzali et al. (1996). Consistently low values of $M(^{56}\mathrm{Ni})$ are also suggested in order to reproduce the observed fluxes and linewidths in that work.

The rapid luminosity decline of SN 1991bg at early epochs is unique, and is indicative of a small ejecta mass (Filippenko et al. 1992; Leibundgut et al. 1993). If the envelope is small, the diffusion time is short and the trapping of the γ-rays from the radioactive decay of ^{56}Ni is less efficient. Therefore, the envelope cools more rapidly, the photosphere recedes faster in mass coordinates and the luminosity decline is faster.

With the noticeable exception of few peculiar SNe (e.g. SN 1988Z, Turatto et al. 1993b), the late-time light curve of SNe is powered by the radioactive decay of ^{56}Co into ^{56}Fe, with an e-folding time of 111 d. The decline rate actually observed depends on the fraction of energy deposited. In the massive SNe II the envelope is for at least 2 yr optically thick to the hard radiation originating in the decay and the luminosity decline rate, ~ 1.0 mag $\times (100\,\mathrm{d})^{-1}$, closely matches the radioactive input. Instead, in SNe Ia the envelope becomes progressively more transparent to the γ-rays and the observed luminosity decline is steeper than the radioactive energy release. In normal SNe Ia a decline rate of 1.5 mag $\times (100\,\mathrm{d})^{-1}$ is observed (Turatto et al. 1990). The very fast decline rate observed in SN 1991bg [2.5 mag $\times (100\,\mathrm{d})^{-1}$] is probably due to the small envelope mass.

Eventually, the envelope becomes transparent to γ-rays and only the kinetic energy of the positron (about 5 per cent of the total decay energy) is deposited. At this point, the light curve is expected to approach the ^{56}Co decline rate. Indeed, a significant flattening of the light curve is indicated by the last observations of SN 1991bg. The observations available allow only a setting of an upper limit to the late decline rate [≤ 1.2 mag $\times (100\,\mathrm{d})^{-1}$]. This is consistent with the ^{56}Co input.

Few other SNe Ia have been observed at phases later than 500 d. One of these was SN 1937C. This SN, although showing a flattening in the photographic light curve around day 300, had a steeper decline rate [1.31 mag $\times (100\,\mathrm{d})^{-1}$] until day 600 (Schaeffer 1994). The case of SN 1992A is different. For this SN recent *HST* observations indicate a flattening of the light curve after day 600 to a rate slower than the ^{56}Co decay rate, suggesting additional energy sources such as ^{44}Ti decay, ionization freeze-out or light echoes. In the case of SN 1991T observed at late phases, a light echo began to influence the light curve and caused it to decline considerably slower than would be expected from ^{56}Co decay (Schmidt et al. 1995). This possibility for SN 1991bg cannot be excluded by current observations.

The main spectral peculiarities of SN 1991bg in the photospheric epoch are the low photospheric expansion velocity, the red colour and the presence of the absorption band between 4200 and 4500 Å. It is shown by Mazzali et al. (1996) that these features can be satisfactorily reproduced if the SN is underluminous and if the abundance of the iron-group elements above 3500 km s^{-1} is low compared with the standard W7 model. An overabundance of Ti with respect to other intermediate-mass elements is not required in order to explain the $\lambda\lambda$4200–4500 feature, which is the result of the low ionization due to the low luminosity.

The peculiarities of the late-time spectra of SN 1991bg with respect to other SNe Ia are highlighted in Fig. 9. The SNe are plotted from top to bottom in sequence of increasing linewidths. It is interesting to note that the objects define also a sequence of absolute magnitudes. In Table 5 we list the absolute magnitudes at maximum, the value of $\Delta m_{15}(B)$, the photospheric velocity at maximum as derived from the Si II line (which may be an overestimate of the actual value, cf. Patat et al. 1996) and the FWHM of the [Co III] lines in the late-time spectra between days 200 and 270. The [Co III] line has been measured because it may be less affected by blending than other lines, e.g. [Fe II] and [Fe III], but the same trend holds also for other emission lines in the nebular spectrum.

A relation between the peak luminosity and the rate of decline, with faster fading SNe Ia being fainter, was first suggested by Pskovskii (1967) and has recently been confirmed on the basis of accurate CCD photometry (Phillips 1993; Hamuy et al. 1995). The trend is well illustrated by the SNe in Table 5, which are a subsample of those of Phillips (1993). From Table 5 we also note that the correlation extends also to the photospheric expansion velocities at maximum and to the expansion velocities of the innermost layers as deduced from the linewidths of the iron-peak elements. The very small velocity in SN 1991bg suggests that in this SN complete nuclear burning was confined to the innermost regions. In other words, observations indicate that SNe Ia with more slowly expanding ejecta, in particular SN 1991bg, have a more rapid photometric evolution and reach a fainter absolute magnitude than rapidly expanding objects.

Arnett (1982) has shown how the ^{56}Ni mass is directly proportional to the square of the velocity scale of expansion. Both the low photosphere and nebular velocities therefore point directly to a low mass of Ni produced in SN 1991bg. Nevertheless, the quantification of this finding is beset by difficulties in defining observationally which velocity should be used. At early phases, because of the great strength of the Si II line, a photospheric velocity is not well defined, while at the late phases the velocities from the widths of the emission lines refer to material concentrated in the innermost parts of the exploding star.

A number of possible explosion scenarios have been proposed to explain the peculiar characteristics of SN 1991bg, and in general the faint SNe Ia.

Hoflich et al. (1995) used delayed detonation models to explain SNe Ia light curves. They argued that, depending on the density at which the transition from deflagration to detonation occurs, different ^{56}Ni masses and, therefore, SNe Ia of different luminosity can be produced by the same explosion mechanism in a Chandrasekhar mass C–O white dwarf (WD). In particular, their PDD5 model, which produces 0.12 $M_\odot$ of ^{56}Ni, gives the best fit to the SN 1991bg observations. In this model the ^{56}Ni is strongly concentrated in the centre, as indicated also by our observations, and a major fraction of the mass is in intermediate-mass elements, with only about 0.05 $M_\odot$ of unburned C/O left after the explosion. However, this model requires a large reddening, $E(B-V)=0.03$, in order to reconcile the predicted luminosity with the observed value, while observations indicate a much smaller value, $E(B-V)=0.05$ (cf. Section 3.2). Also,

the decline rates of the PDD5 model are similar to those of their standard Ia model (N32), while we found SN 1991bg to be faster (cf. Section 3).

An alternative scenario for faint SNe Ia was proposed by Livne (1990) and Woosley & Weaver (1994). In their models a C–O WD with mass below the Chandrasekhar limit accretes He at a rate of the order of a few 10^{-8} $M_\odot$ yr^{-1} until He ignites at the bottom of the layer. The in-going shock wave induces a detonation of the C–O which disrupts the star. According to Woosley & Weaver (1994) less-mass WDs produce smaller ^{56}Ni masses and less energy, in qualitative agreement with our findings. The lower mass WD results in a larger fraction of intermediate-mass elements and an overproduction of other isotopes (including Ti^{44}) in the He detonation layer, while a large fraction of He is left unburned. We already noted, however, that an overproduction of ^{44}Ti is not required by the spectral synthesis models. The visibility of He in the ejecta is not expected because of the observed low temperatures. Moreover, the models of Mazzali et al. (1996) seem to exclude the short risetimes to maximum light (of the order of 13 d) which are obtained by Woosley & Weaver (1994). These subChandrasekhar models produce in the interior a nearly constant velocity as a function of mass and, therefore, they do not reproduce the low velocities observed in SN 1991bg at late stages.

In another explosion mechanism, proposed by Nomoto et al. (1996), a low mass of ^{56}Ni is produced by the collapse of an O–Ne–Mg WD formed after the merging of a double C–O WD system. In order to reproduce the observed luminosity the collapsing core has to be embedded in a C–O envelope of 0.6 $M_\odot$, and the shock wave propagating through it produces 0.15 $M_\odot$ of ^{56}Ni, compatible with the estimates found above. The resulting light curve reproduces satisfactorily the observed one in the first 100 d but Si seems to be located at velocities too high to reproduce the observed lines.

Unfortunately the observations alone do not suggest unambiguously a preferred model for the progenitor. All suffer from the various difficulties discussed above. Mazzali et al. (1996) show through modelling that even in the most promising models one has to resort to ad hoc adjustments of abundances and their stratification to approximate the observed spectra. Thus SN 1991bg has provided an additional challenge to our understanding of the Type Ia supernova phenomena.

7 CONCLUSIONS

The new observations presented in this paper confirm the peculiar characteristics of SN 1991bg and give new insights into its late-time behaviour.

In particular, SN 1991bg was fainter than normal SNe Ia by about 2.5 mag in the *B* band, but by less than 2 mag in the *V* band, thus giving a particularly red colour at maximum, $(B-V)_{max}=0.74$. However, because of a different colour evolution, the SN turned to the colour curve of normal SNe Ia already 40–50 d later. The rates of decline in all optical bands (*BVRI*) are at all epochs the most rapid ever observed in SNe Ia (Table 3). The constructed *uvoir* bolometric light curve is consequently steeper than in the normal SN Ia SN 1992A. A very deep *V*-band observation obtained 530 d past maximum showed that before this epoch the fading rate had decreased to about 1.2 mag $\times$ $(100\,d)^{-1}$, and we stress that, on the basis of the available data, energy sources other than Co decay are not required.

The low luminosity at maximum is an indication that the SN produced a small mass of Ni (<0.2 $M_\odot$), whereas the fast photometric evolution was related to a small mass of the envelope. The small explosion energy also causes the photosphere at maximum light to be cooler than in typical SNe Ia, as is evident when comparing the early-time spectra. This also explains the broad absorption feature between 4200 and 4500 Å identified with Ti II, which has been attributed to an ionization effect by Mazzali et al. (1996).

A peculiarity of the spectrum of SN 1991bg at epochs subsequent to maximum is the presence of the two narrow features at about 5700 Å (in absorption) and 5900 Å (in emission). The absorption lacks, at the moment, a convincing explanation mainly because there is no significant evolution redwards, while the emission, which appeared already on day 34, is plausibly an early emergence of [Co III] in accordance with the fast evolution to the nebular stage shown by SN 1991bg. It has been noted that the spectrum of SN 1991bg evolved to the nebular stage earlier than usual.

Contrary to previous claims, the overall appearance of the spectrum maintained a general resemblance to those of other SNe Ia at least until 200 d after maximum light (Fig. 9), indicating that the ionization conditions of the iron core were similar to those of other SNe Ia at this phase. In particular, there has been no sudden change in the nature of the spectrum during the interval day 143 to day 203. Nevertheless, the emission lines were exceptionally narrow, and allowed the identification of the main emissions with lines of [Fe II], [Fe III] and [Co III]. The presence of hydrogen at late times seems unlikely.

The small photospheric expansion velocity and envelope mass, combined with the small expansion velocity and mass of the iron-group core, as seen from the late-time spectra and luminosity, point to a kinetic energy smaller than in typical SNe Ia. We pointed out that the correlation between the luminosity at maximum and the early rate of decline can be extended also to the expansion velocities of the photosphere at maximum and to the innermost layers emitting the nebular spectrum (Table 5). In other words, the luminosity at maximum correlates to the kinetic energy of the SNe Ia.

One important question is whether the lower energy SN 1991bg can be considered an extreme case of a continuous distribution of SNe Ia or whether it is a representative of a separate subclass of faint SNe Ia. We reviewed the literature and found that while a handful of other SNe Ia shared some of the observed characteristics of SN 1991bg, none was quite so extreme. This may support the concept of a continuum transition from faint SNe Ia (SN 1991bg-like) to *normal* ones. Obviously, a continuum of SNe Ia properties might jeopardize their use as standard candles, at least until one understands better the inter-relation between light curves and spectral characteristics.

ACKNOWLEDGMENTS

We thank Roberto Rampazzo and Caterina Zanin for obtaining some of the observations reported in this paper.

This work has been conducted as part of the ESO Key

Programme on Supernovae, and based on observations collected at ESO La Silla, Chile and Asiago, Italy.

REFERENCES

Arnett W. D., 1982, in Supernovae: A Survey of Current Research. Reidel, Dordrecht, p. 221
Arnett W. D., Branch D., Wheeler J. C., 1985, Nat, 314, 337
Barbon R., Ciatti F., Rosino L., 1973a, A&A, 25, 241
Barbon R., Ciatti F., Rosino L., 1973b, Mem. Soc. Astron. It., 44, 65
Barbon R., Benetti S., Cappellaro E., Rosino L., Turatto M., 1990, A&A, 237, 79
Benetti S., Cappellaro E., Turatto M., 1991, IAU Circ. 5405
Branch D., 1984, in Evans D. S., ed., XI Texas Symposium on Relativistic Astrophysics. NY Academy of Science, 422, 186
Branch D., 1992, ApJ, 392, 35
Burstein D., Heiles C., 1984, ApJS, 54, 33
Cappellaro E., Turatto M., Benetti S., Tsvetkov D. Yu., Bartunov O. S., Makarova I. N., 1993, A&A, 273, 383
Cappellaro E., Turatto M., Fernley J., 1995, Supernovae, IUE–ULDA Access Guide N.6, ESA SP-1189, Noordwijk
Ciardullo R., Jacoby G. H., Tonry J. L., 1993, ApJ, 419, 479
Cristiani S. et al., 1992, A&A, 259, 63
Filippenko A. V. et al., 1992, AJ, 104, 1543
Frogel J. A., Gregory B., Kawara K., Phillips M. M., Laney D., 1987, ApJ, 315, L129
Gomez G., Lopez R., 1995, AJ, 109, 737
Hamuy M. et al., 1994, AJ, 108, 2226
Hamuy M., Phillips M. M., Maza J., Suntzeff N. B., Schommer R. A., Aviles R., 1995, AJ, 109, 1
Hoflich P., Khokhlov A. M., Wheeler J. C., 1995, ApJ, 444, 831
Hoflich P., Khokhlov A. M., 1996, ApJ, 457, 500
Kikuchi S., 1971, PASJ, 23, 593
Kosai H., Kushida R., Kushida H., Kato T., 1991, IAU Circ. 5400
Kuchner M. J., Kirshner R. P., Pinto P. A., Leibundgut B., 1994, ApJ, 426, L89
Landolt A. U., 1992, AJ, 104, 340
Leibundgut B. et al., 1993, AJ, 105, 301
Livne E., 1990, ApJ, 354, L53
Maza J., Hamuy M., Phillips M. M., Suntzeff N., Aviles R., 1994, ApJ, 424, L107
Mazzali P. A., Danziger I. J., Turatto M., 1995, A&A, 297, 509
Mazzali P. A., Chugai N., Turatto M., Lucy L., Danziger I. J., Cappellaro E., Della Valle M., Benetti S., 1996, MNRAS, in press
Meyerott R. E., 1980, ApJ, 239, 257
Nomoto K., Thielemann F. K., Yokoi K., 1984, ApJ, 286, 644
Nomoto K., Yamaoka H., Shigeyama T., Iwamoto K., 1996, in McCray R., Wang Z., eds, Supernova and Supernova Remnants. Cambridge Univ. Press, Cambridge, p. 49
Patat F., Benetti S., Cappellaro E., Danziger I. J., Della Valle M., Mazzali P., Turatto M., 1996, MNRAS, 278, 111
Phillips M. M., 1993, ApJ, 413, L105
Phillips M. M., Well L. A., Suntzeff N. B., Hamuy M., Leibundgut B., Kirshner R. P., Foltz C. B., 1992, AJ, 103, 1632
Porter A. C., Dickinson M., Stanford S. A., Lada E. A., Fuller G. A., 1992, BAAS, 24, 1244
Pskovskii Y. P., 1967, SA, 11, 63
Pskovskii Y. P., 1971, SA, 14, 798
Ruiz-Lapuente P., Cappellaro E., Turatto M., Gouiffes C., Danziger I. J., Della Valle M., Lucy L. B., 1992, ApJ, 387, L33
Ruiz-Lapuente P. et al., 1993, Nat, 365, 728
Saha A., Sandage A., Labhardt T., Schwengeler H., Tammann G. A., Panagia N., Macchetto F. D., 1995, ApJ, 438, 8
Sandage A., Tammann G. A., 1993, ApJ, 415, 1
Schaeffer B. E., 1994, ApJ, 426, 493
Schmidt B. P., Kirshner R. P., Leibundgut B., Wells L. A., Porter A. C., Ruiz-Lapuente P., Challis P., Filippenko A. V., 1995, ApJ, 434, L19
Suntzeff N. B., 1996, in McCray R., Wang Z., eds, Supernova and Supernova Remnants. Cambridge Univ. Press, Cambridge, p. 41
Tully R. B., 1988, Nearby Galaxy Catalog. Cambridge Univ. Press, Cambridge
Turatto M., Cappellaro E., Barbon R., Della Valle M., Ortolani S., Rosino L., 1990, AJ, 100, 771
Turatto M., Cappellaro E., Benetti S., Danziger I. J., 1993, MNRAS, 265, 471
Turatto M., Cappellaro E., Benetti S., 1994, AJ, 108, 202
Vaughan T. E., Branch D., Miller L., Perlmutter S., 1995, ApJ, 439, 558
Wheeler J. C., Benetti S., 1996, in Cox A. N., ed., Astrophysical Quantities, IVth edn. In press
Woosley S. E., Weaver T. A., 1994, ApJ, 423, 371